CDF/ANAL/ELECTROWEAK/CDFR/xxxx
12 Feb 2010

Measurement of the Foward-Backward Asymmetry A_{fb} in Dimuon Drell-Yan Events

Arie Bodek, YeonSei. Chung, JiYeon Han, Kevin .S. McFarland, Willis K. Sakumoto, and Alex Strelnikov
University of Rochester

ABSTRACT

Drell-Yan dimuon pairs are produced in the process, $p\bar{p} \rightarrow \gamma^* Z + X$, with the subsequent decay of the γ^*/Z into lepton pairs (l^+l^-). We study the Foward-Backward Asymmetry A_{fb} of the angular distribution of dimuon events using 6.4 fb^{-1} of CDF Run II data, and compare to the CDF Monte Carlo and other theory predictions. We extract the electroweak mixing angle from the data.

1 Quarks bound in a nucleon

When quarks are bound in the nucleon, the dilepton can be produced with non-zero transverse momentum. For $p\bar{p}$ or pp collisions the angular distribution of γ^*/Z vector bosons decaying to e^+e^- or $\mu^+\mu^-$ pairs is given by:

$$\frac{d\sigma}{d(\cos\theta)} \propto [1 + \cos^2\theta + h(\theta)] + A_4 \cos\theta \quad (1)$$

$$h(\theta) = \frac{1}{2} A_0(M_{\ell\ell}, P_T)(1 - 3\cos^2\theta) \quad (2)$$

The $q\bar{q}$ center of mass frame is well defined when the lepton pair has zero transverse momentum (P_T). For a non-zero transverse momentum of the dilepton pair, the $q\bar{q}$ center of mass frame is approximated by the Collins-Soper frame[1].

When integrated over all of $\cos\theta$ the $h(\theta)$ term integrates to zero and the forward backward asymmetry is given ben $A_{fb} = (3/8)\ A_4$. However, when there is only a partial acceptance over a limited range of $\cos\theta$, the integrated asymmetry depends on the $\cos\theta$ range and on the $h(\theta, M_{\ell\ell}, P_T)$ (or A_0) term.

The term $h(\theta, M_{\ell\ell}, P_T)$ is a small QCD correction term which is zero when the transverse momentum of the dilepton pair is zero.

For quark-antiquark annihilation the angular coefficient A_0 is only a function of the dilepton mass ($M_{\ell\ell}$) and transverse momentum (P_T) and is given by:

$$A_0^{\bar{q}q} = \frac{P_T^2}{P_T^2 + M_{\ell\ell}^2} \quad (3)$$

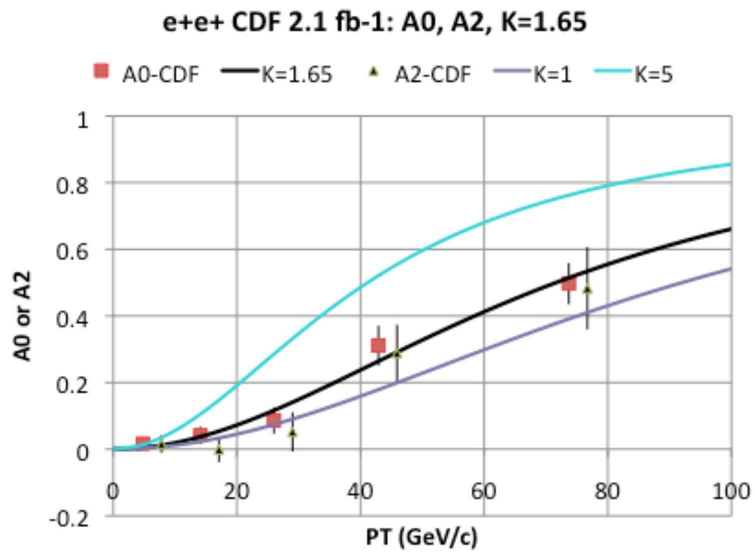

Figure 1: Comparison of the fit $A_0^{CDF} = \frac{KP_T^2}{KP_T^2+M_{\ell\ell}^2}$ to the CDF 2.1 fb^{-}1 data in the e^+e^- channel (dilepton mass region 66-116 GeV/c^2. K = 1.65 ± 0.3 is fits the data.

For the quark-Gluon Compton process an approximate expression for the angular coefficient A_0 as a function of the dilepton mass ($M_{\ell\ell}$) and transverse momentum (P_T) and is given by:

$$A_0^{qG} \approx \frac{5P_T^2}{5P_T^2 + M_{\ell\ell}^2} \tag{4}$$

In general, for a combination of both quark-antiquark and quark-Gluon diagrams we can describe the data by the form:

$$A_0 = \frac{KP_T^2}{KP_T^2 + M_{\ell\ell}^2} \tag{5}$$

The CDF Tevatron results[2] for A_0 and A_2 function of the dilepton mass ($M_{\ell\ell}$) and transverse momentum (P_T) are shown in Fig. 1. These were extracted from the first 2.1 fb^{-} $e+e-$ sample of run II. For $\bar{q}q$ processes K=1, and for qG processes, K is approximately equal to 5. The data are integrated over the Z mass region (66-116 GeV) . As shown in the figure, the $e+e-$ data are described by K=1.65 ±0.3 This implies that Z production at the Tevatron involves a combination of both $\bar{q}q$ (K=1) and qG (K≈ 5) processes. The data are in agreement with the predictions of POWHEG, DYRAD and other fixed order perturbation theory calculations. It is also in agreement with RESOBS.

In contrast, the CDF default PYTHIA MC is described with K=1. This occurs because the modeling of the qG processes in the default PYTHIA MC is incomplete.

For the specific case of the $\cos\theta$ event weighting technique, when we do an analysis of data events we use $K = 1.65$ and when we do an analysis of PYTHIA MC events in

CDF we use K=1. In the extraction of A_{bf} and A_4 integrated over all P_T this does not make much difference. However, when we study A_4 versus P_T, it makes a small difference in the high P_T bins.

2 Simple (conventional) versus event weighting in $\cos\theta_{cs}$

There are two ways of extracting A_{fb} and A_4 , the simple (conventional way), and the event weighting technique. The conventional way is

$$A_{fb}^{total} = \frac{\sigma_f - \sigma_b}{\sigma_b + \sigma_b} = \frac{3}{8}A_4 \quad (6)$$

For full acceptance in $\cos\theta_{cs}$ the term in A_0 integrate to zero. However, when we have a limited range of $\cos\theta_{cs}$, there are angular acceptance corrections which depends on the detector acceptance and on A_0. These must be determined from MC and depend both on the physics model, and on the detector acceptance.

At a fixed mass and y, the event weighting techniques automatically corrects for the $\cos\theta_{cs}$ acceptance of the detector. The only corrections which remain in order to determine the true A_{fb} and A_4 are corrections for detector resolution and final state radiation. These corrections can also be determined from MC, but are smaller.

If we extract A_{fb} and A_4 over a range of mass and y, then the detector acceptance as a function of mass and y needs to be corrected for. Although the dependence on y is small, the correction for the y acceptance can be minimized for extractions of A_{fb} and A_4 for fixed range of y which is within the detector acceptance, thus eliminating the need to extrapolate to large y (e.g. $|y| < |$ for dimuon events).

If the mass distribution in data and MC is the same, then the modeling of the *relative* acceptance versus mass is well understood. As mentioned earlier, in $\cos\theta_{cs}$ event weighting technique, the absolute acceptance in mass and $\cos\theta_{cs}$ cancels in A_{fb} and A_4 . This is important in the analysis of dimuon events for which the angular acceptance of the detector is limited.

For dimuon events, the acceptance is complicated function of detector η and $\phi$and difficult to model precisely. The $\cos\theta_{cs}$ event weighting technique has the advantage that it does not depend on the angular acceptance of the detector. In addition, the event weighting technique results in the reduction of the error in A_{fb} by a factors of 1.2 to 1.4.

3 Simple (conventional) analysis

We begin by discussing the conventional way of doing the asymmetry analysis. If N_f is in number of events in the forward direction of the quark and N_b is the number of events in the backward direction of the quark we obtain the following expression for

Source	$M_{\mu\mu} \in [70,110]$	$M_{\mu\mu} \in [110,130]$	$M_{\mu\mu} > 130$
Z/γ^*	146498.4	1903.6 ± 190	1797.0 ± 90.0
WW	38.0 ± 3.8	11.1 ± 0.5	21.6 ± 1.1
$t\bar{t}$	28.1 ± 2.8	11.2 ± 0.6	24.0 ± 1.2
MisID	46.6 ± 2.4	5.7 ± 0.2	8.1 ± 0.4
Cosmics	0.7 ± 0.02	0.1 ± 0.01	0.05 ± 0.01
Total	146611	1932 ± 192.0	1850.7 ± 90
Data	146382	1982	1813

Figure 2: Table from a previous analysis of CDF dimuon sample (taken from CDF/ANAL/EXOTIC/CDFR/10070), showing that the background in the Z mass region is of order 100 events our of 140,000. Here, MisID refers to background form QCD jets.

the total forward backward-asymmetry (A_{fb}^{total}) and its error (ΔA_{fb}^{total}):

$$[A_{fb}] = \frac{N_f - N_b}{N_f + N_b} = \frac{N_f - N_b}{N} = \frac{3}{8}A_4 \tag{7}$$

$$\tag{8}$$

$$\frac{N_f}{N_b} = \frac{1 - A_{fb}^{total}}{1 + A_{fb}^{total}}$$

$$N_f = \frac{1 + A_{fb}^{total}}{2}N$$

$$N_b = \frac{1 - A_{fb}^{total}}{2}N$$

$$\Delta A_{fb} = \frac{2}{N}\left[\frac{N_f N_b}{N}\right]^{1/2} = \frac{3}{8}\Delta A_4 \tag{9}$$

$$\Delta A_{fb} = \left[\frac{1 - (A_{fb(expected)})^2}{N}\right]^{1/2} = \frac{3}{8}\Delta A_4 \tag{10}$$

where we have used $\Delta N_f = (N_f)^{1/2}$ and $\Delta N_b = (N_b)^{1/2}$, and $N = N_f + N_b$. Since for Poisson statistics the fractional error is $(1/N_{expected})^{1/2}$ and not $(1/N_{observed})^{1/2}$, we use $A_{fb(expected)}$ in equation 10. For $\bar{p}p$ collisions above the Z mass peak (for a full $\cos\theta_{cs}$ acceptance) $A_{fb(expected)}$=0.6. In this region, $\Delta A_{fb} = 0.800 \cdot (1/N)^{1/2}$.

4 Correcting for background in the simple analysis

In a previous analysis of CDF dimuon sample, the backgrounds in the Z mass region (66-116 GeV) are very small (of order 100 events out of 140,000), as shown in Fig. 2 taken[3] from CDF/ANAL/EXOTIC/CDFR/10070. Nonetheless, this is how they affect the analysis.

In the simple analysis, we correct for background in the following way.

$$A_{corr}(M) = \frac{(N_f - B_f) - (N_b - B_b)}{(N_f - B_f) + (N_b - B_b)} \tag{11}$$

where $B_f = N_{f\ expected}^{background}$, and $B_b = N_{b\ expected}^{background}$. We also define the total number events $N = N_f + N_b$, the total number of background events $B = B_f + B_b$, and the fractional backgrounds $\delta = B/N$, $\delta_f = B_f/N_f$ and $\delta_b = B_b/N_b$.

We treat the errors on the background as systematic errors. However, even if the background is very well known, the background still changes the statistical error in the corrected asymmetry as follows:

$$\Delta A_{corr} = \frac{2}{(N-B)} \left[\frac{N_f(N_b - B_b)^2 + N_b(N_f - B_f)^2}{(N-B)^2} \right]^{1/2} \tag{12}$$

$$\Delta A_{corr} = \frac{2}{N(1-\delta)} \left[\frac{N_f N_b^2 (1-\delta_b)^2 + N_b N_f^2 (1-\delta_f)^2}{N^2(1-\delta)^2} \right]^{1/2} \tag{13}$$

$$\Delta A_{corr} \approx \frac{2}{N(1-\delta)} \left[\frac{N_f N_b}{N} \right]^{1/2} \tag{14}$$

In the last line we made the approximation that $\delta \approx \delta_f \approx \delta_b$. Note that the error is larger than if we just assumed that the background educed the statistical sample by a factor of $(1-\delta)$. This simplified assumption yields

$$\Delta A_{reduced\ statistics} = \frac{2}{N-B} \left[\frac{(N_f - B_f)(N_b - B_b)}{N-B} \right]^{1/2} \tag{15}$$

$$\Delta A_{reduced\ statistics} \approx \frac{2}{N(1-\delta)^{1/2}} \left[\frac{N_f N_b}{N} \right]^{1/2} \tag{16}$$

Which means that we can obtain a simple formula for the increase in the statistical error due to background (from what is given in equation 9).

$$\Delta A_{corr} \approx \Delta A^2_{reduced\ statistics} / \Delta A_{fb} \tag{17}$$

where

$$\Delta A_{fb} = \frac{2}{N} \left[\frac{N_f N_b}{N} \right]^{1/2} = \left[\frac{1 - (A_{fb(expected)})^2}{N} \right]^{1/2} \tag{18}$$

Since the background is about 100 out of 140,000. The correction to the asymmetry is negligible and the increase in the error is negligible,

5 The angle event weighting technique

As mentioned eralier, when quarks are bound in the nucleon, the dilepton can be produced with non-zero transverse momentum. For $p\bar{p}$ or pp collisions we write the angular distribution of γ^*/Z vector bosons decaying to e^+e^- or $\mu^+\mu^-$ pairs as:

$$\frac{d\sigma}{d(\cos\theta)} \propto [1+\cos^2\theta + h(\theta)] + A_4\cos\theta \tag{19}$$

$$h(\theta) = \frac{1}{2}A_0(M_{\ell\ell}, P_T)(1-3\cos^2\theta) \tag{20}$$

Each event has a measured value of $|c_j| = |\cos\theta_j|$. Since the angular distribution is know, if we bin the events in bins of $|c_j| = |\cos\theta_j|$, we can get a measurement of A_4 from each $\cos\theta$ bin and average all the measurements of A_4. Then we can use A_{fb} = (3/8) A_4 to get A_{fb} . The event weighting technique is equivalent to binning in $\cos\theta$, but is also valid for the case of low statistics. The expressions for combining events with different $|c_j| = |\cos\theta_j|$ and values to yield the best average value of A_{fb} asymmetry are derived in Ref. **??** . The expressions are:

$$z_{1,j} = \frac{1}{2}\frac{c_j^2}{(1+c_j^2+h(\theta,P_T))^3} \tag{21}$$

$$z_{2,j} = \frac{1}{2}\frac{|c_j|}{(1+c_j^2+h(\theta,P_T))^2}$$

$$N_{total} = \sum_{all-events}[1]$$

$$A1 = \sum_{forward-events}[z_{1,j}] \tag{22}$$

$$A2 = \sum_{back-events}[z_{1,j}] \tag{23}$$

$$B1 = \sum_{forward-events}[z_{2,j}] \tag{24}$$

$$B2 = \sum_{back-events}[z_{2,j}] \tag{25}$$

$$[\Delta A1]^2 = \sum_{forward-events}\left[z_{1,j}^2\right]$$

$$[\Delta A2]^2 = \sum_{back-events}\left[z_{1,j}^2\right]$$

$$[\Delta B1]^2 = \sum_{forward-events}\left[z_{2,j}^2\right] \tag{26}$$

$$[\Delta B2]^2 = \sum_{back-events}\left[z_{2,j}^2\right] \tag{27}$$

$$A = A1 + A1$$

$$B = B1 - B2$$

$$[A_{fb}]^{raw} = \frac{3}{8}\frac{B}{A} = \frac{3}{8}\frac{B1-B2}{A1+A2}$$

$$\begin{aligned}
\Delta A1 &= \Delta B1 \cdot \frac{A1}{B1} \\
\Delta A2 &= \Delta B2 \cdot \frac{A2}{B2} \\
\left[\Delta A_{fb}^{raw}\right]^2 &= \left[\frac{3}{8}\right]^2 \frac{1}{(A1+A2)^4}\left[E1^2 + E2^2\right] \\
E2^2 &= \frac{[\Delta B_1]^2}{B1^2}(A2B1 + A1B2)^2 \\
E2^2 &= \frac{[\Delta B_2]^2}{B2^2}(A2B1 + A1B2)^2
\end{aligned}$$

Here N_{total} is the total number of events. Note that since we add up the forward and backwards events in separate sums, the weighting factors $z_{1,j}$ and $z_{2,j}$ are functions of the absolute value $|\cos\theta|$.

The $|\cos\theta|$ event weighting takes care of most of the $|\cos\theta|$ acceptance and efficiencies. We still need to subtract the very small background (e.g. QCD, Cosmic Rays, and EW (e.g $\tau^+\tau^-$, $\bar{t}t$, WW, WZ, ZZ), as described below.

In addition, we need to correct for resolution smearing, FSR/radiative corrections and the fact that the asymmetry is a function of y and the acceptance of the detector is a function of y. We show in an appendix. that corrections for resolution, FSR/radiative effects can be treated the same as correcting for backgrounds.

6 Correcting for background in the angle event weighting technique

As mentioned earlier the background in the Z mass region (66-116 GeV) is about 110 events out of 140,000. Nonetheless, this is how they affect the analysis

In the simple analysis, we correct for background in the following way. $A_{corr}(M)$ is just a ratio $(N^f_{corr} - N^b_{corr})/(N^f_{corr} + N^b_{corr})$, where $N^f_{corr} = N^f - N^{f\ expected}_{background}$, and $N^b_{corr} = N^b - N^{b\ expected}_{background}$. We will treat the errors on the background as systematic errors. Here the backgrounds are the sum of the background from all sources.

For each specific source of background, we have Monte Carlo samples of forward (f) and backward (b) background events. The background samples need to be normalized to the integrated luminosity of the data by a factor F.

$$N^{expected}_{back} = F \sum_{all-events} [1] \quad (28)$$

$$A1_{background} = F \sum_{forward-background-events} [z_{1,j}] \quad (29)$$

$$A2_{background} = F \sum_{back-background-events} [z_{1,j}]$$

$$B1_{background} = F \sum_{forward-background-events} [z_{2,j}]$$

$$
\begin{aligned}
B2_{background} &= F \sum_{back-background-events} [z_{2,j}] \\
[\Delta B1]^2_{background} &= F \sum_{forward-background-events} \left[z^2_{2,j}\right] \\
[\Delta B2]^2_{background} &= F \sum_{back-background-events} \left[z^2_{2,j}\right]
\end{aligned}
$$

For each background, we remove the background contributions of to $A1$, $A2$, $B1$, $B2$, $[\Delta B1]^2$, and $[\Delta B2]^2$ for *each* of the sources of background, e.g. QCD, EW (top, $\tau^+\tau^-$ etc), cosmic rays, and charge misID (charge misID can be treated as a background or a dilution since it is very small). This calculation yields the asymmetry corrected for background, and the error in the asymmetry that we get is the reduced statistics error.

$$
\begin{aligned}
A1_{corr} &= A1 - A1_{all-backgrounds} \\
A2_{corr} &= A2 - A2_{all-backgrounds} \\
B1_{corr} &= B1 - B1_{all-backgrounds} \\
B2_{corr} &= B2 - B2_{all-backgrounds} \\
[\Delta B1]^2_{corr} &= [\Delta B1]^2 - [\Delta B1]^2_{all-backgrounds} \\
[\Delta B2]^2_{corr} &= [\Delta B2]^2 - [\Delta B2]^2_{all-backgrounds} \\
[A_{corr}] &= \frac{3}{8}\frac{B1_{corr} - B2_{corr}}{A1_{corr} + A2_{corr}} \\
[\Delta A_{reduced-statistics}]^2 &= \left[\frac{3}{8}\right]^2 \frac{1}{(A1_{corr} + A2_{corr})^4} \left[E1^2_{corr} + E2^2_{corr}\right] \\
E2^2_{corr} &= \frac{[\Delta B1_{corr}]^2}{B1^2_{corr}} (A2_{corr}B1_{corr} + A1_{corr}B2_{corr})^2 \\
E2^2_{corr} &= \frac{[\Delta B2_{corr}]^2}{B2^2_{corr}} (A2_{corr}B1_{corr} + A1_{corr}B2_{corr})^2 \\
[\Delta A_{corr}] &= [\Delta A_{reduced-statistics}]^2 / \Delta A^{raw}_{fb}
\end{aligned} \tag{30}
$$

The systematic error in the background is determined by varying the level of the background sample F^f and F^b for each background source (within its error).

7 Effect of CTC Alignment on A_{fb}

The electron analysis uses the energy in the calorimeter to determine the mass of the dilepton pair. Since the calibration of positrons and electrons in the calorimeter is the same, there is no sensitivity to the alignment of the CTC. The CTC is only used to determine the sign of the forward or backward leptons.

For dimuons, the momentum is determined from the tracker. In CDF, the direction of the proton and antiproton is fixed, and the magnet polarity is not changed (unlike

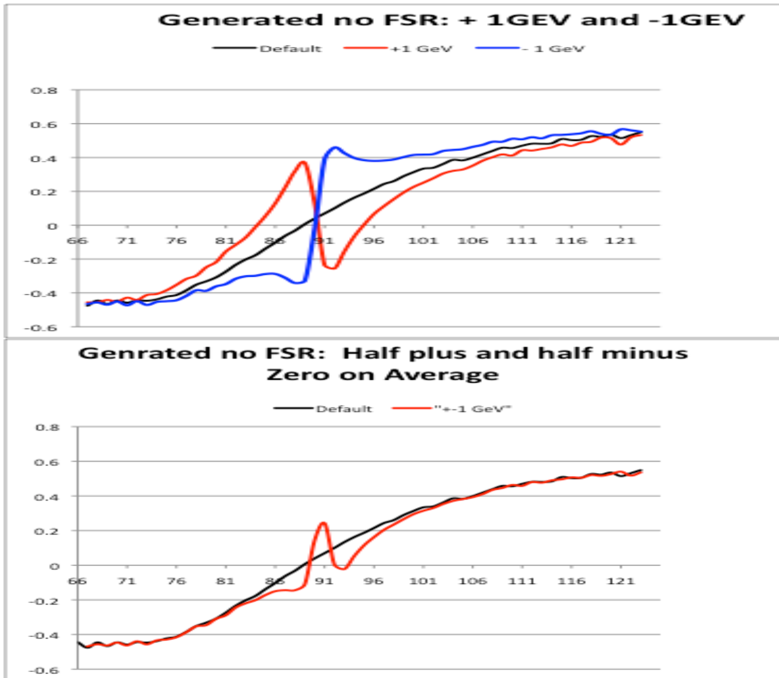

Figure 3: MC at the generated level (no FSR). Top: Change in the nominal A_{fb} (black) resulting from a plus (red) and minus (blue) one GeV shift in mass between positive and negative $\cos\theta_{cs}$ events. Bottom: Change in the nominal A_{fb} (black) when half the events shifted by +1 GeV and the other half are shifted by -1 GeV.

Dzero which changes their magnet polarity to check for systematics). Therefore, a CTC misalignment which may be different between positive and negative $\cos\theta_{lab}$ can result in a shift in the mass distribution which is different for positive versus negative $\cos\theta_{cs}$ events.

The top of Fig.3 shows what happens at the generator level (no FSR) to the nominal A_{fb} (black) for a plus (red) and minus (blue) one GeV calibration difference in the mass distribution between positive and negative $\cos\theta_{cs}$ events. The bottom of the figure shows what happens to the nominal A_{fb} (black) when half the events are shifted by +1 GeV and the other half are shifted by -1 GeV (shown in red) . This indicates that even if on average, the mass distribution is unbiased, the details of the asymmetry as a function of mass are affected (though the average asymmetry integrated over the entire Z mass region remains unchanged).

8 The dimuon data sample and cuts

We use 6.5 fb^{-}1 of dimuon data. The cuts that we use are:

1. $66 < M_{\ell\ell} <$116 GeV/c^2

2. Data uses Larry's Tuning
3. Opposite sign
4. Had energy < 6 + .028*max(0,p-100)
5. Calorimeter Isolation Et/Pt < .1
6. EM energy < 2 + .0115*max(0,p-100)
7. >=3 axial superlayers with >=5 hits
8. >=2 stereo superlayers with >= 5 hits
9. abs(d0) <2mm
10. COT abs(z0) <60cm
11. CMU abs(delX) <7cm
12. CMP abs(delX) <5cm
13. CMX abs(delX) ¡<6cm
14. Both muons have pt > 20
15. Allowed Topologies: CMUP tight-CMUPtight,CMUPtight-CMX,CMX-CMX,CMUPloose-CMUPtight,CMUPloose-CMX

9 Momentum Calibration of Data and MC as a function of $\cos\theta$ and ϕ in the lab frame.

Fig. 4 shows A_{fb} as a function of dimuon mass for data as compared to default CDF PYTHIAMC. Here, A_{fb} is extracted using the $\cos\theta_{cs}$ event weighting technique for both data and MC events. Our default is that the momentum in the data is corrected using Larry's corrections since the CTC in the data is misaligned. The momenta in MC are in general not corrected with Larry's correction since the CTC in the MC is not misaligned. On the top figure, the data has Larry's CTC momentum correction (as it should), and the reconstructed MC does not (as it should). In the bottom figure the data has Larry's CTC $P_T$correction (as it should), and as a test of the magnitude of Larry's correction, we also apply Larry's correction to the MC (in practice, this should not be done).

What we observe in Fig. 4 (top) is that there are mis-calibrations in both data and MC. What we observe from the test in Fig. 4 (bottom) is that Larry's momentum correction has a large effect on A_{fb} .

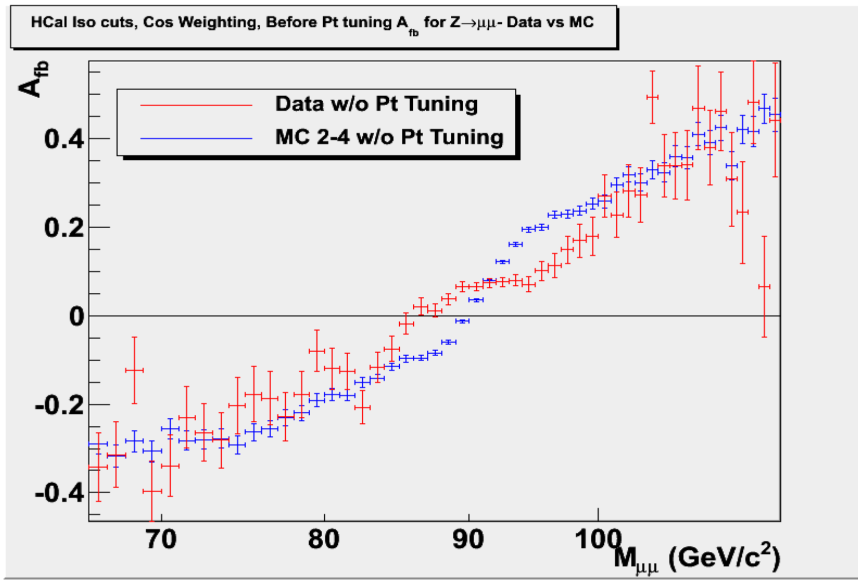

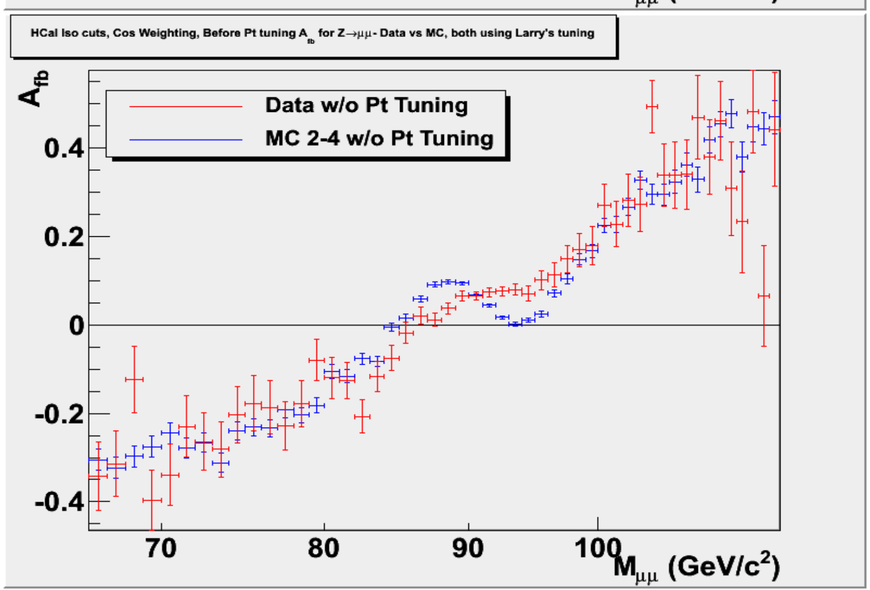

Figure 4: A_{fb} as a function of dimuon mass for data as compared to MC. On the top figure, the data has Larry's CTC momentum correction (as it should) and the reconstructed MC does not (as it should). In the bottom figure the data has Larry's CTC P_T correction (as it should), and as a test of the magnitude of Larry's correction, we also apply Larry's correction to the MC (in practice, this should not be done).

MC			**ACCEPTED**	
<1/pt->/<1/pt+>			**GENERATED**	
	1.0026	1.0082	1.0073	1.0043
	0.9998	1.0021	1.0029	1.0017
	0.9990	0.9993	0.9999	0.9997
	0.9935	0.9928	0.9964	0.9962
Ratio	errors			
	0.0002	0.0002	0.0001	0.0001
	0.0001	0.0001	0.0001	0.0001
	0.0001	0.0001	0.0001	0.0001
	0.0001	0.0001	0.0001	0.0002

MC			**ACCEPTED**	
<1/pt->/<1/pt+>			**RECONSTRUCTED**	
	1.0384	**0.9895**	1.0019	**1.0537**
	1.0140	0.9968	**0.9837**	1.0018
	1.0058	1.0061	**0.9782**	**0.9773**
	1.0036	**1.0109**	**0.9883**	**0.9791**
Ratio	errors			
	0.0002	0.0002	0.0001	0.0001
	0.0001	0.0001	0.0001	0.0001
	0.0001	0.0001	0.0001	0.0001
	0.0001	0.0001	0.0001	0.0002

DATA				
<1/pt->/<1/pt+>			**DATA**	
	0.9985	1.0032	1.0009	1.0027
	0.9923	1.0024	0.9980	1.0200
	0.9956	**0.9888**	0.9930	**1.0246**
	1.0023	**0.9694**	**0.9798**	**1.0384**
Ratio	errors			
	0.0039	0.0047	0.0045	0.0040
	0.0018	0.0021	0.0023	0.0024
	0.0013	0.0021	0.0024	0.0022
	0.0041	0.0043	0.0035	0.0037

Figure 5: Top: The ratio of $\langle 1/\ P_T \rangle$ for positive and negative muons in MC for the generated momenta (after FSR) for accepted events. The ratio is very close to 1, as it should be, with small differences due to acceptance effects. Middle: The ratio of $\langle 1/\ P_T \rangle$ for positive and negative muons in MC for the reconstructed momenta. The deviations which are larger than 1% are shown in red. Bottom: The ratio of $\langle 1/\ P_T \rangle$for positive and negative muons in data. If there is no bias in the data, these ratios should be the same as for the generated MC events. The deviations which are larger than 1% are shown in red.

We now proceed to determine the addition momentum tuning to correct for the remaining mis-calibrations in data and MC. We determine these momentum tuning correction in a 4×4 grid in $\cos\theta$(lab) and ϕ(lab).

Fig. 5 (top) we show the ratio of $\langle 1/P_T{}^- \rangle$ for negative muons and $\langle 1/P_T{}^+ \rangle$ for positive muons calculated using generated momenta (post FSR) all of the accepted events. The four rows are bins in ϕ and the four columns are bins in $\cos\theta$. The ratio is very close to 1, as it should be, with minor differences due to small acceptance effects.

Fig. 5 (middle) shows the ratio of $\langle 1/P_T{}^- \rangle$ for negative muons and $\langle 1/P_T{}^+ \rangle$ for positive muons using the reconstructed momenta of MC events. If there is no bias in the MC, the ratios for the reconstructed quantities should be the same as for the generated quantities. The deviations which are larger than 1% are shown in red. There are 10 regions (out of 16) in the $\cos\theta$ and ϕ grid for which the deviations are larger than 1%, and some are larger than 5%.

Fig. 5 (bottom) shows the ratio of $\langle 1/P_T{}^- \rangle$ for negative muons and $\langle 1/P_T{}^+ \rangle$ for positive muons for the the data. The bottom part of the figure If there were no bias in the data, these ratios should be the same as for the generated MC events. The deviations which are larger than 1% are shown in red. There are four regions (out of 16) in $\cos\theta$ and ϕ which have deviations which are larger than 1%.

We now apply the additional $P_T$tuning as follows. We find the mean $\langle 1/\ P_T{}^- \rangle$ and $\langle 1/\ P_T{}^+ \rangle$ for positive and negative muons, respectively in each of the 16 $\cos\theta$ and ϕ using the generated momenta (post FSR) for MC accepted events. We also find the means using the reconstructed momenta for MC accepted events, and do the same for data events. We then apply multiplicative factors to data and reconstructed MC events to make the means of reconstructed MC, and reconstructed data the same as for the generated quantities.

The top part of Fig. 6 shows a comparison of A_{fb} for MC reconstructed events before (blue) and after (red) the additional P_T tuning. The additional $P_T$tuning results in a significant change in A_{fb} as a function of mass. The bottom part of the figures shows a comparison of A_{fb} for MC reconstructed after the additional tuning (blue) compared to A_{fb} for the same events using the generated variables (red). There is good agreement between the generated A_{fb} and reconstructed A_{fb} in the region of the Z mass. Note that momentum resolution smearing of events from Z peak to lower and higher masses is expected to result in a reconstructed asymmetry which is slightly lower than the generated asymmetry for masses higher than the Z peak and a reconstructed asymmetry which is slightly lower than the generated asymmetry for masses lower than the Z peak

The top part of Fig. 7 shows a comparison of A_{fb} for data events before (blue) and after (red) the additional P_T tuning. The additional $P_T$tuning results in only a small change in A_{fb} in data as a function of mass. The bottom part of the figures shows a comparison of A_{fb} for the data after the additional tuning (red) compared to A_{fb} for reconstructed MC events after $P_T$tuning (blue).

The additional $P_T$tuning results in good agreement in A_{fb} between data and MC as a function of mass. Note that neither Larry's momentum correction, nor the additional $P_T$tuning change A_{fb} and A_4 for the integrated sample between 66-116

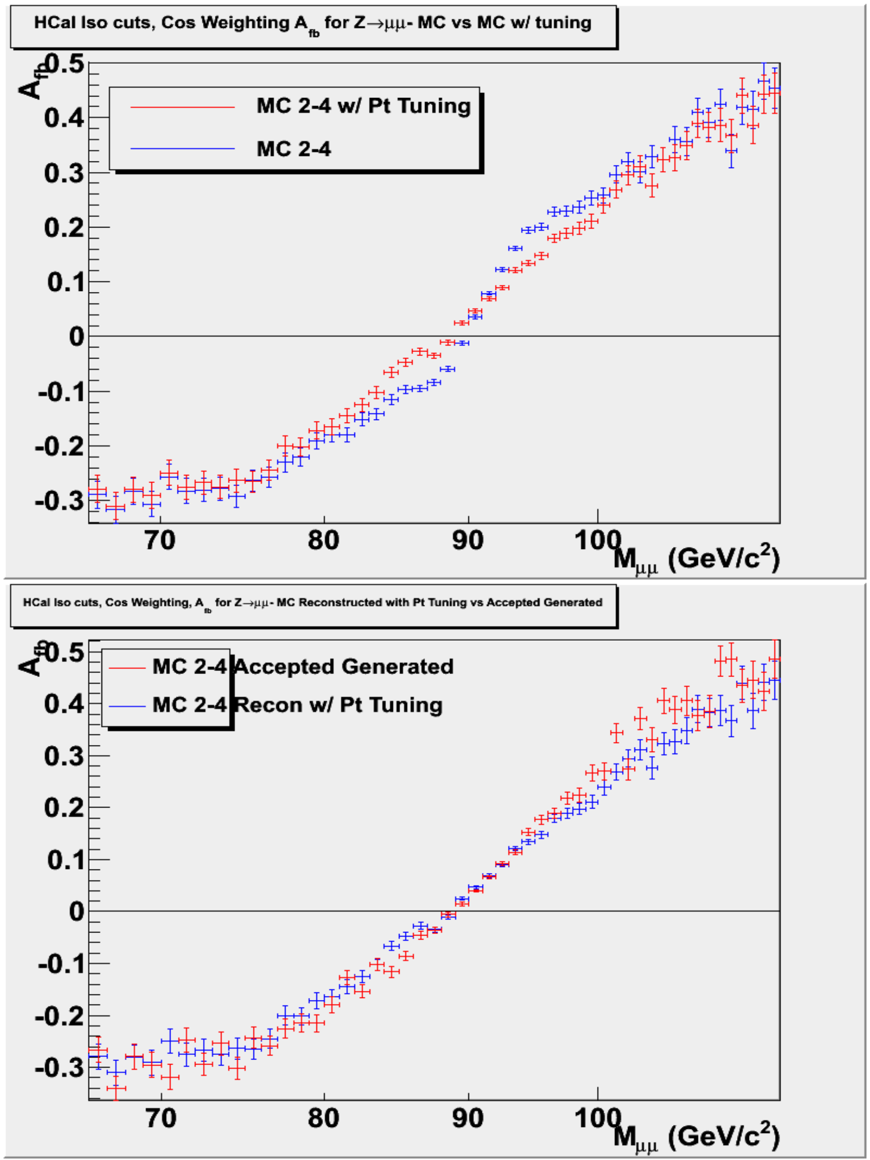

Figure 6: Top: A comparison of A_{fb} for MC reconstructed events before (blue) and after (red) the additional P_T tuning. The additional $P_T$tuning results in a significant change in A_{fb} as a function of mass. Bottom: A comparison of A_{fb} for MC reconstructed with the additional $P_T$tuning correction (blue) to A_{fb} calculated for the same events, but using the generated (post FSR) momenta. There is good agreement between the generated A_{fb} and reconstructed A_{fb} in the region of the Z mass. Note that momentum resolution smearing of events from Z peak to lower and higher masses is expected to result in a reconstructed asymmetry which is slightly lower than the generated asymmetry for masses higher than the Z peak and a reconstructed asymmetry which is slightly lower than the generated asymmetry for masses lower than the Z peak.

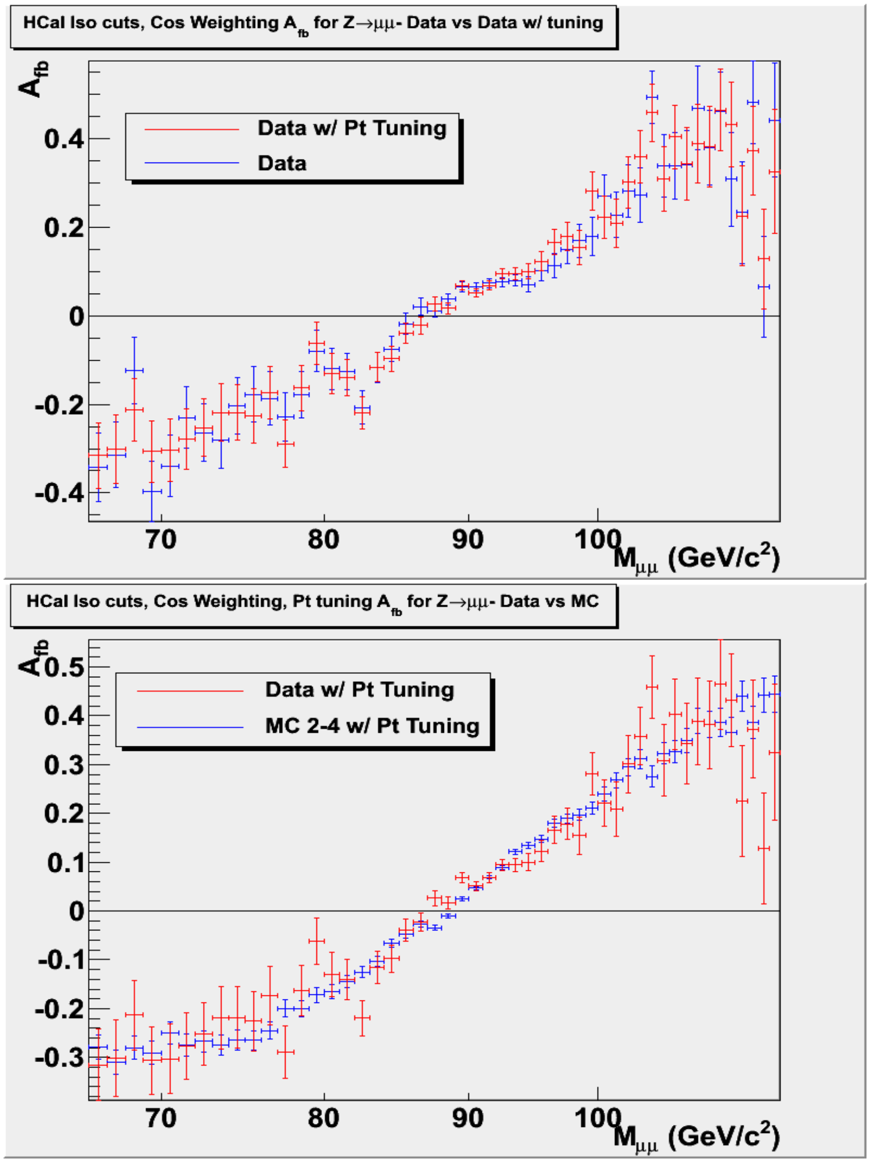

Figure 7: Top: A comparison of A_{fb} for data events before (blue) and after (red) the additional P_T tuning. The additional $P_T$tuning results in a small change in measured A_{fb} as a function of mass. Bottom: A comparison of A_{fb} for the data after the additional $P_T$tuning (red) compared to A_{fb} for reconstructed MC events after the additional $P_T$tuning (blue).

GeV. This is because the tuning does not move events from positive to negative $\cos\theta$. Therefore, in order to avoid any sensitivity to momentum tuning corrections, we prefer to extract average values of A_{fb} and A_4 values integrated over the Z mass region (e.g. 66-116) in the extraction of the electroweak mixing angle from the data. These average values are completely insensitive to $P_T$tuning corrections

Similarly, In the measurement of the unfolded A_{fb} in the muon channel, we plan to use only 3 wide mass bins bin in the Z mass region (66-80, 80-100, and 100-116 GeV)For masses larger than 116 GeV, the sensitivity of A_{fb} to momentum tuning and calibration is small (because the change of A_{fb} as a function of mass is small).

10 Appendix: Theory of Angular Distributions

The parton level differential cross sections for dilepton pair production (e.g. Drell-Yan, $Z's$ or $W's$) for $q\bar{q}$ annihilation can be written as

$$\frac{d\sigma}{d(\ cos\theta)} = C\left[(1+cos^2\theta) + B\ cos\theta\right] \tag{31}$$

where θ is the emission angle of the positive charged lepton relative to the quark momentum in the center of mass frame. For W and Z bosons B is a parameter that depend on the weak isospin and charge of the incoming fermions (B=2 for W bosons). The cross sections for forward events (σ_f) and backward events (σ_b) are given by

$$\begin{aligned}\sigma_f &= \int_0^1 \frac{d\sigma}{d(\ cos\theta)} d(\ cos\theta) \qquad (32)\\ &= C\left[\left(1+\frac{1}{3}\right) + B\left(\frac{1}{2}\right)\right]\\ \sigma_b &= \int_{-1}^0 \frac{d\sigma}{d(\ cos\theta)} d(\ cos\theta) \qquad (33)\\ &= C\left[\left(1+\frac{1}{3}\right) - B\left(\frac{1}{2}\right)\right]\end{aligned}$$

The electroweak interaction introduces the asymmetry (a linear dependence on $cos\theta$), which can be expressed as

$$A_{fb}^{total} = \frac{\sigma_f - \sigma_b}{\sigma_b + \sigma_b} = \frac{3}{8}B \tag{34}$$

The total differential cross sections dilepton pair production (e.g. Drell-Yan, $Z's$ or $W's$) for proton-antiproton annihilation [5, 6, 7, 8, 9] is given by a modified equation:

$$\frac{d\sigma}{dP_T^2 dy d\cos\theta d\phi} = C[(1+\cos^2\theta)$$

$$
\begin{aligned}
&+ \quad \frac{1}{2}A_0(1-3\cos^2\theta) + A_1 \sin 2\theta \cos\phi \\
&+ \quad \frac{1}{2}A_2 \sin^2\theta \cos 2\phi + A_3 \sin\theta\cos\phi \\
&+ \quad A_4 B \cos\theta + A_5 \sin^2\theta \sin 2\phi \\
&+ \quad A_6 \sin 2\theta \sin\phi + A_7 \sin\theta \sin\phi] \qquad (35)
\end{aligned}
$$

where P_T and y are the transverse momentum and the rapidity of the *dilepton* in the lab frame and θ and ϕ are the polar and azimuthal angles of the charged lepton from the *dilepton* decay in the Collins-Soper (CS) frame [1].

For reference we present other notations that is used in the literature. If we sum up negative and positive values of $cos\theta$ and integrate over ϕ some papers use:

$$\frac{d\sigma}{dP_T^2 dy d\cos\theta} = C(1+\frac{A_0}{2})[1+\alpha_2\cos^2\theta + \alpha_1\cos\theta] \qquad (36)$$

where

$$\alpha_2 = \lambda = \frac{2-3A_0}{2+A_0}, \qquad A_0 = \frac{2(1-\lambda)}{3+\lambda}, \qquad \alpha_1 = \frac{2A_4}{2+A_0}$$

and also

$$\frac{d\sigma}{dP_T^2 dy d\cos\theta d\phi} = C'(\frac{1}{\lambda+3})[1+\lambda\cos^2\theta + \mu\ sin2\theta\cos\phi + \frac{\nu}{2}\sin^2\theta\cos 2\phi] \qquad (37)$$

$$\lambda = \frac{2-3A_0}{2+A_0}, \qquad \mu = \frac{2A_1}{2+A_0}, \qquad \nu = \frac{2A_2}{2+A_0}$$

And we integrate over $cos\theta$, some papers use:

$$\frac{d\sigma}{dP_T^2 dy d\phi} = C''[1+\beta_1\cos\phi + \beta_2\cos 2\phi + \beta_3\sin\phi + \beta_4\sin 2\phi] \qquad (38)$$

where

$$\beta_1 = \frac{3\pi A_3}{16}, \quad \beta_2 = \frac{A_2}{4}, \beta_3 = \frac{3\pi A_7}{16}, \quad \beta_4 = \frac{A_5}{4}$$

When integrated over all ϕ the differential cross section reduces to:

$$\frac{d\sigma}{dP_T^2 dy d\cos\theta} = C[(1+\cos^2\theta) + \frac{1}{2}A_0(1-3\cos^2\theta) + A_4\cos\theta] \qquad (39)$$

The angular coefficients are non-zero for finite values of P_T, A_0 and A_2 and are the same for virtual photons and Z exchange processes. The coefficients A_3 and A_4 originate from the interference terms. For P_T=0 all the angular coefficients are zero, except for A_4.

the $q\bar{q}$ process ($q + \bar{q} \rightarrow \gamma^*/Z + g$), the non-zero transverse momentum originates from gluon emission by the $q\bar{q}$ initial state. For the qg process ($q + g \rightarrow \gamma^*/Z + q$), the boson P_T originates from a non-zero transverse momentum recoil of the quark in the final state.

For the $q\bar{q}$ process, perturbative calculations show that the coefficients A0, A2 are independent of y and independent of the parton distribution functions. They originate from pure kinematics and are related to ξ , which is the angle of the proton (antiproton) beam in the Collins-Soper frame as follows:

$$A_0^{q\bar{q}} = A_2 = sin^2\ \xi = \frac{P_T^2}{P_T^2 + M_{\ell\ell}^2} \tag{40}$$

For the $q\bar{q}$ process, the above relations remain the same in resummation calculations [11].

The angular coefficient A_0 for the qg diagram was calculated in LO by Linfors in 1979 publication, [13]. When integrated over all y, A_0 and A_2 for the qg can be approximated by:

$$A_0^{q\bar{q}} = A_2 = \frac{5P_T^2}{5P_T^2 + M_{\ell\ell}^2} \tag{41}$$

The relation $A_0 = A_2$ which is equivalent to $1 - \lambda - 2\nu = 0$, is known as the Lam-Tung(LT) relation. It is valid to all orders for the $q\bar{q}$. At LO it was shown that it is still true for the sum of $q\bar{q}$ and qg. This relationship is only valid for spin 1/2 gluons. The qg diagram at higher orders leads to a small violation of the LT relation[6, 7] (it makes A_2 a little smaller than A_0.

In this CDF note we focus on the measurement of A_4. For a fixed CM energy, A_0 is a function of the dilepton mass, P_T and rapidity, and depends on the electroweak mixing angle. The reason it is a function of rapidity is that A_4 has one sign when it is a results of processes involving quarks in the proton. When the processes involves sea-antiquarks in the proton, A_4 has the opposite sign. Therefore, the antiquark fraction dilutes the measured value of A_4 . At the the fraction of events originating from the sea-antiquarks in the proton is small. However, the fraction of sea-anitquark induced events it is a function of rapidity (it becomes smaller at larger rapidity).

The angular coefficients A_0, A_2, A_3 and A_4 were measured in the e^+e^-channel for the dilepton mass range of 66 to 116 GeV/c^2 as shown in Figure 1.

The electron data shows that there at non-zero transverse momentum, the data are described by a combination of qq and qG diagrams. The parametrization

$$A_0^{CDF} = \frac{K\ P_T^2}{K\ P_T^2 + M_{\ell\ell}^2} \tag{42}$$

with K=1.65±0.3 provides a good description of the data as shown in Figure 2. This indicates a combination of qq (K=1) and qG (K=5) processes. In contrast, the CDF default The PYTHIA MC is described with K=1, indicating the the modeling of the qG processes is incomplete.

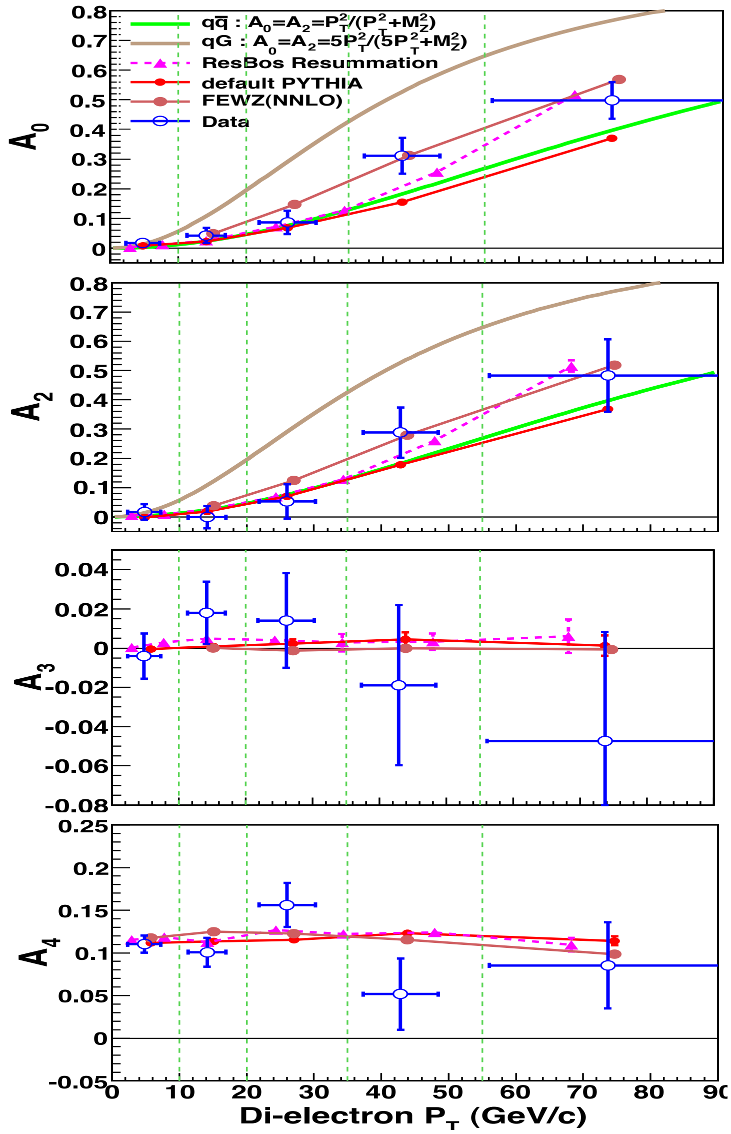

Figure 8: The angular coefficents A_0, A_2, A_3 and A_4 as measured in the e^+e^- channel with 2.1 fb^{-1} for the dilepton mass range of 66 to 116 GeV/c^2

Therefore, when we do an analysis of data events we use $K = 1.65$ and when we do an analysis of PYTHIAMC events we use K=1. In analysis of A_{bf} and A_4 integrated over all P_T this does not make much difference. However, it makes a small difference in the high P_T bins when we study A_4 versus P_T.

11 Appendix: Unfolding (correcting for resolution smearing and FSR)

In the analysis of the data using $\cos\theta_{cs}$ weighting, we primarily compare the data to a smeared post FSR Monte Carlo. In this case, no unfolding needs to be done. Similarly, the A_{fb} and A_4 integrated over the Z mass region (66-116) are insensitive to resolution effects.

However, if we want to present unfolded A_{fb} corrected for resolution smearing and FSR, we need to include unfolding into the event weighting technique.

In the simple analysis, corrections for resolution and FSR are typically done using a martix inversion technique. However, in the event weighting technique, the events that smear out of a mass bin, do not affect the asymmetry in a mass bin, they just reduce the statistics. Therefore, no correction need to be made for events that smear out of the bin due to FSR and resolution smearing. Events which smear into a mass bin change the measured asymmetry. The simplest way to handle these events is to treat them as background.

When we treat the FSR and resolution smearing as a background, the statistical errors increase. In addition, we need to include the systematic error in the FSR and resolution smearing background.

We run the full MC, and for each bin we generate a sample of events that come into a bin from outside the bin (either from resolution smearing, or from FSR). The number of such events in each bin is labeled $N^i_{smear-in}$. We do not care where the events come, or for what reason (FSR or resolution). We also keep track of the number of events that remained in each bin N^i_{remain}

The MC sample of events that smear into each bin is a background and is treated as any other background. The background sample is normalized to the data by a factor $N^i_{data}/(N^i_{smear-in} + N^i_{remain},$

References

[1] J.C. Collins and D.E. Soper, Phys. Rev. **D16**, 2219 (1977).

[2] Measurement of the Angular Coefficients of Drell-Yan e+e? pairs in the Z Mass Region from pp? Collisions at s = 1.96 TeV. CDF Collaboration (T. Aaltonen (Helsinki Inst. of Phys.) et al.). FERMILAB-PUB-11-153-E. Mar 2011. 7 pp. Submitted to: Phys.Rev. Lett. e-Print: arXiv:1103.5699 [hep-ex]

[3] Search for high mass resonances decaying to muon pairs Author(s): D. Whiteson, E. Quinlan, K. Cranmer, A. Kotwal, C. Hays, O. Stelzer-Chilton CDF Note Number: CDF/ANAL/EXOTIC/CDFR/10070 Date: 2/7/10

[4] A simple event weighting technique for optimizing the measurement of the forward-backward asymmetry of Drell-Yan dilepton pairs at hadron colliders. Arie Bodek, Eur.Phys.J.C67:321-334,2010 e-Print: arXiv:0911.2850 [hep-ex]

[5] E. Mirkes, Nucl. Phys. B **387** 3, (1992).

[6] W and Z polarization effects in hadronic collisions. E. Mirkes , J. Ohnemus, Phys. Rev. **D50**:5692-5703 (1994).

[7] Angular distributions of Drell-Yan lepton pairs at the Tevatron: Order α_s^2 corrections and Monte Carlo studies. E. Mirkes , J. Ohnemus, Phys. Rev. **D51**:4891-4904 (1995). e-Print: hep-ph/9412289

[8] Study of the angular coefficients and corresponding helicity cross sections of the W boson in hadron collisions. John Strologas, Steven Errede, Phys. Rev. **D73**:052001 (2006).

[9] Measurement of the Differential Angular Distribution of the W Boson produced in association with Jets in Proton - Anti-proton Collisions center-of-mass energy = 1.8-TeV. John Strologas, (Illinois U., Urbana) . FERMILAB-THESIS-2002-47, UMI-30-70054, Dec 2002. 259pp. Ph.D. Thesis (Advisor: Steven Errede).

[10] J. C. Collins, Phys. Rev. Lett. **42**, 291 (1979); Daniel Boer and Werner Vogelsang, Phys. Rev. **D74**:014004 (2006).

[11] Edmond L. Berger,, Jian-Wei Qiu, , Ricardo A. Rodriguez-Pedraza, Phys. Rev. **D76**:074006 (2007): Edmond L. Berger , Jian-Wei Qiu, Ricardo A. Rodriguez-Pedraza, Phys. Lett. **B656** (2007).

[12] W production in an improved parton shower approach. Gabriela Miu, Torbjorn Sjostrand, Phys. Lett. **B449**:313-320 (1999).

[13] J. Lindfors, Physica Scripta **20**, 19 (1979).

[14] T. Sjöstrand et al., Comput. Phys. Commun. **135**, 238 (2001). PYTHIA 6.2: hep-ph/0108264.

[15] T. Sjöstrand et al., JHEP **05**, 026 (2006). PYTHIA 6.4: hep-ph/0603175.